New Phytologist

Research

Elevated CO_2 increases R gene-dependent resistance of *Medicago truncatula* against the pea aphid by up-regulating a heat shock gene

Yucheng Sun[1]*, Huijuan Guo[1]*, Erliang Yuan[1,2] and Feng Ge[1,2]

[1]State Key Laboratory of Integrated Management of Pest Insects and Rodents, Institute of Zoology, Chinese Academy of Sciences, Beijing 100101, China; [2]University of Chinese Academy of Sciences, Beijing 100049, China

Author for correspondence:
Feng Ge
Tel: +8610 6480 7123
Email: gef@ioz.ac.cn

Received: *19 June 2017*
Accepted: *11 October 2017*

New Phytologist (2017)
doi: 10.1111/nph.14892

Key words: *Acyrthosiphon pisum*, elevated CO_2, feeding behavior, heat shock gene, *Medicago truncatula*, R gene.

Summary

- Resistance against pathogens and herbivorous insects in many plant results from the expression of resistance (R) genes. Few reports, however, have considered the effects of elevated CO_2 on R gene-based resistance in plants.
- The current study determined the responses of two near isogenic *Medicago truncatula* genotypes (Jester has an R gene and A17 does not) to the pea aphid and elevated CO_2 in open-top chambers in the field.
- Aphid abundance, mean relative growth rate and feeding efficiency were increased by elevated CO_2 on A17 plants but were reduced on Jester plants. According to proteomic and gene expression data, elevated CO_2 enhanced pathogen-associated molecular pattern (PAMP)-triggered immunity (PTI) but decreased the effector-triggered immunity (ETI) in aphid-infested A17 plants. For aphid-infested Jester plants, by contrast, elevated CO_2 enhanced the ETI-related heat shock protein (HSP) 90 and its co-chaperones, the jasmonic acid (JA) signaling pathway, and ubiquitin-mediated proteolysis. In a loss-of-function experiment, silencing of the HSP90 gene in Jester plants impaired the JA signaling pathway and ubiquitin-mediated proteolysis against the aphid under ambient CO_2, and negated the increased resistance against the aphid under elevated CO_2.
- Our results suggest that increases in expression of HSP90 are responsible for the enhanced resistance against the aphid under elevated CO_2.

Introduction

Global atmospheric CO_2 concentrations have been increasing at an accelerating rate and are expected to reach 550–950 ppm by the end of this century (IPCC, 2013). The typical effects of elevated CO_2 on plants include increases in photosynthetic rate, biomass and carbon : nitrogen (C : N) ratio (Ainsworth & Rogers, 2007). The assimilation and allocation of C and N resources within plant tissues under elevated CO_2 inevitably alters the primary and secondary metabolites of host plants, which in turn affects the performance of herbivorous insects. Previous studies and meta-analysis have shown that sap-sucking insects are essentially the only feeding guild to consistently show positive effects under elevated CO_2 (Robinson *et al.*, 2012). The explanations may include their exclusive feeding on phloem sap, which is a long-term adaptation to an extremely high C : N ratio diet, and specialized feeding behavior to interact with the host plants. Aphids, for example, generally exhibit increased fecundity, abundance and survival under elevated CO_2 (Pritchard *et al.*, 2007; Robinson *et al.*, 2012). There is substantial evidence that the positive effects of elevated CO_2 on aphids result from changes in host plant resistance and nutritional components. Regarding resistance, several studies have reported that elevated CO_2 suppresses the jasmonic acid (JA)/ethylene (ET) signaling pathways of host plants and thereby enhances the feeding efficiency and performance of herbivorous insects (Zavala *et al.*, 2013).

To resist attack by pathogens or herbivorous insects, plants activate their immune system and modulate the defense signaling network (Pieterse *et al.*, 2012). When attacked by pathogens, plants typically recognize pathogen-associated molecular patterns (PAMPs) and induce PAMP-triggered immunity (PTI) (Bittel & Robatzek, 2007). When attacked by aphids and other phloem-feeding insects, plants can recognize molecules in the insect saliva and activate early events of PTI defenses such as mitogen-activated protein kinase (MAPK), calcium influx and release of reactive oxygen species (ROS) via the membrane receptor BRI1-ASSOCIATED KINASE1/SOMATIC EMBRAYOGENESIS (BAK1/SERK); these early responses subsequently activate SA signaling pathways to provide local defense (Hogenhout & Bos, 2011; Chaudhary *et al.*, 2014; Jaouannet *et al.*, 2014). On the

*These authors contributed equally to this work.

other hand, successful pathogens or phloem-feeding insects can actively suppress the PTI defenses by delivering effector molecules into the host. During the long-term arms race between plant and insect or pathogen, some biotypes of host plants acquired monogenic resistance genes (R genes), including nucleotide-binding site–leucine-rich repeat (NBS-LRR) genes; the proteins encoded by these genes recognize the effectors of the targeted attacker, resulting in effector-triggered immunity (ETI). Compared to PTI, ETI confers more efficient, prolonged and robust resistance against target insects (Stuart *et al.*, 2012). To date, a number of R genes have been identified that confer resistance in cultivated crops against sap-sucking insects including aphids, the Hessian fly, brown planthoppers and whiteflies (Ratcliffe *et al.*, 1994; Nombela *et al.*, 2003; Klingler *et al.*, 2005; Du *et al.*, 2009). Although research has shown the ETI may involve the JA signaling pathway and hypersensitive responses (Gao *et al.*, 2007), the underlying regulatory mechanism and signaling are mostly unclear.

Most studies on the effects of elevated CO_2 on plant resistance against sap-sucking insects have focused on PTI defenses in plants that lack R genes, that is, in plants that lack ETI defenses. In these studies, elevated CO_2 typically suppressed the efficient JA/ET-mediated resistance but up-regulated the inefficient salicylic acid (SA) signaling-mediated resistance against aphids and thereby increased aphid feeding efficiency (Sun *et al.*, 2013; Guo *et al.*, 2014b). Few studies, by contrast, have determined the effects of elevated CO_2 on R gene-mediated ETI defenses. In one such study, R gene-dependent resistance in red raspberry against the European large raspberry aphid was reduced by elevated CO_2, suggesting that elevated CO_2 may suppress R gene-mediated defenses of host plants against aphids (Martin & Johnson, 2011). Because both PTI and ETI involve downstream phytohormone-dependent signaling pathways (Tsuda & Katagiri, 2010), the effects of elevated CO_2 on phytohormone-dependent defensive pathways in R gene-containing plants should be studied, as such information will help to elucidate the R gene-mediated ETI defenses against target aphid under future CO_2-enriched environments.

R gene-dependent resistance can be modified by abiotic factors such as drought, salinity and temperature (Williamson, 1998; Chini *et al.*, 2004; Heidrich *et al.*, 2012). For example, R gene-mediated resistance against root-knot nematodes in tomato is nullified when soil temperatures exceed 28°C (Williamson, 1998). In another example, heat stress reduces disease resistance in *Arabidopsis* by reducing R protein accumulation in the nucleus and downstream signal transduction (Zhu *et al.*, 2010; Mang *et al.*, 2012). Furthermore, the stability of R protein structure and the initiation of signal transduction of ETI defenses require a particular subclass of heat-shock proteins, the cytosolic heat shock protein 90 (HSP90). HSP90 contributes to the maintenance of protein complexes and the degradation of misfolded peptides under abiotic stress conditions (Schulze-Lefert, 2004; Song *et al.*, 2009; Nishizawa-Yokoi *et al.*, 2010). Researchers have therefore proposed that HSP90 could help regulate the activation and maintenance of R gene-dependent resistance against pathogens or insects in response to abiotic stress conditions (Kissoudis *et al.*, 2014). Because previous transcriptomic data showed that elevated CO_2 up-regulated two HSP90 genes in *Arabidopsis* (Li *et al.*, 2008), we speculated that a change in the expression of HSP90 genes under elevated CO_2 could affect R gene stability and R gene-dependent defenses of plants.

Two R genes, Acyrthosiphon kondoi resistance (AKR) and Acyrthosiphon pisum resistance (APR), have been identified in the Jester genotype of *Medicago truncatula*. AKR confers resistance against the blue green aphid *Acyrthosiphon kondoi* (Klingler *et al.*, 2005; Gao *et al.*, 2008), while APR confers resistance against the Australian biotype of the pea aphid *Acyrthosiphon pisum*. The downstream defensive signaling pathway in Jester plants, however, seems to differ in response to these two aphid species (Gao *et al.*, 2007, 2008). Furthermore, Jester plants with the APR gene have efficient resistance against certain *A. pisum* biotypes from Australia but are susceptible to several clones from Europe, suggesting that ETI defenses in Jester plants are induced by some *A. pisum* biotypes but not by others (Kanvil *et al.*, 2014).

The current study used two *M. truncatula* genotypes that differ in resistance to *A. pisum*. One genotype, Jester, has the APR gene, and the other genotype, A17, is a near-isogenic line that lacks the APR gene. Our specific goals were (1) to determine plant growth traits and aphid performance as affected by plant genotype; (2) to compare protein expression patterns of the two plant genotypes in response to aphid infestation and elevated CO_2; and (3) to identify the key molecules responsible for the plant-mediated effects of elevated CO_2 on aphid performance.

Materials and Methods

Control of CO_2 concentrations

Experiments were performed in eight octagonal, open-top field chambers (OTCs) (4.2 m diameter and 2.4 m height) at the Observation Station of the Global Change Biology Group, Institute of Zoology, Chinese Academy of Science in Xiaotangshan County, Beijing, China (40°11′N, 116°24′E). The CO_2 concentrations were set at the current atmospheric CO_2 concentration (*c.* 400 μl l^{-1}) and at an elevated CO_2 concentration (700 μl l^{-1}, which is that predicted for the end of this century) (IPCC, 2013). Four blocks were used for each of the two CO_2 treatments, and each block contained one pair of OTCs (one with ambient CO_2 and one with elevated CO_2). The CO_2 concentration in each OTC was monitored and adjusted with an infrared CO_2 analyzer (Ventostat 8102; Telaire Co., Goleta, CA, USA). The auto-control system for maintaining the CO_2 concentrations as well as specifications for the OTCs are detailed in Guo *et al.* (2013).

Host plants

The R gene-containing genotype cv Jester and its near-isogenic genotype cv A17 of *M. truncatula* Gaertn. were kindly provided by Professor Wenhao Zhang, State Key Laboratory of Vegetation and Environmental Change, Institute of Botany, Chinese Academy of Sciences, China. Most (89%) of the Jester genome is derived from A17 (Gao *et al.*, 2007). A17 and Jester plants were

grown and inoculated with *Sinorhizobium meliloti* 1021 as described previously (Guo *et al.*, 2013). After they had grown in sterilized soil for 2 wk, the seedlings were individually transplanted into plastic pots (35 cm diameter and 28 cm height) containing sterilized loamy field soil (organic carbon 75 g kg^{-1}, N 500 mg kg^{-1}, P 200 mg kg^{-1}, K 300 mg kg^{-1}) and were placed in OTCs. Each OTC contained 30 plants of each plant genotype (30 plants × 2 plant genotypes × 8 OTCs = 480 plants in total).

Aphid infestation

The pea aphid *A. pisum* was originally collected from *Pisum sativum* L. in Yunnan Province and had been reared in the laboratory for 5 yr at the start of this study (Guo *et al.*, 2013, 2014a). The nymphal instars from the same parthenogenetic female were reared on *Vicia faba* with 14 h (25°C) : 10 h (22°C) light : dark cycle in photoclimate chambers (Safe PRX-450C, Ningbo, China).

After they had grown in the OTCs for 6 wk, the plants were randomly divided into four groups. In the first group, six plants of each genotype per OTC (96 plants in total) were randomly selected for determining the aphid population abundance, and each was infested with five apterous 4^{th}-instar *A. pisum* nymphs. The plants were placed in cages made with 80-mesh gauze, and the nymphs developed and produced offspring freely on each plant for 15 d. Changes in aphid numbers on each plant were determined. Another four plants of each genotype per OT (64 plants in total) were randomly selected for determining the aphid mean relative growth rate (MRGR). Pea aphids were weighed with an automatic electrobalance before and after feeding on *M. truncatula* plants. The MRGR was calculated as previously described (Leather & Dixon, 1984): $MRGR = (\log_e W2 - \log_e W1)/t$, where W1 is the initial weight, W2 is the final weight, and t is the time in days between each weighing.

In the second group, six plants of each genotype per OTC were randomly selected for recording aphid feeding behavior, and each was infested with one apterous *A. pisum* adult for 12 h. The feeding behavior of aphids is described in the next section.

In the third group, four pairs of A17 and Jester plants in each OTC (64 plants in total) were randomly selected for use in choice tests. In each test, 35 adults were released at an equal distance between two plants of different genotypes in mesh cages. Six hours later, the number of adults that had settled on each plant was determined. Each CO_2 concentration was represented by 16 pairs of plants.

In the fourth group, eight plants of each genotype per OTC (128 plants in total) were randomly selected for iTRAQ proteomic analysis (as described in the relevant section below), gene expression analysis and growth traits. Eight of these plants per genotype were infested with 50 apterous 4^{th}-instar nymphs as follows: the nymphs were transferred to five mature trifoliate leaves (the fourth to eighth terminal, mature, trifoliate leaves from the base of the shoot). The infested plants were placed in cages (one plant per cage) constructed with 80-mesh gauze. The other eight plants of each genotype served as the uninfested control and were caged in the same way. After 24 h, the aphids were removed. The damaged leaves of four infested plants and the undamaged leaves of four uninfested plants of each genotype per OTC were collected for iTRAQ proteomic analysis and gene expression analysis.

Another four plants of each genotype per OTC were also caged as uninfested controls. Plants were then harvested for measurement of photosynthetic rate, Chl content, biomass, flower numbers, flowering time after germination and pod numbers according to Guo *et al.* (2013).

Aphid feeding behavior

The electrical penetration graph (EPG) method is useful for monitoring aphid stylet location and activity during probing, salivation into sieve elements and passive uptake of phloem sap (Walker, 2000). The feeding behavior of *A. pisum* on A17 and Jester plants in the second group was studied as described by Guo *et al.* (2014a). Each combination of plant genotype and CO_2 concentration was represented by 24 biological replicates; as noted earlier, one trifoliate leaf on each plant was infested with one apterous adult of *A. pisum*. An eight-channel amplifier was used to simultaneously monitor the feeding of eight aphids on separate plants for 12 h. Adult aphids were immobilized on ice, and then aphid dorsum was attached to a gold wire (2 cm length, 18.5 μm diameter; EPG Systems, Wageningen, the Netherlands) using hand-mixed, water-based silver conducting paint glue (EPG Systems). The other side of the gold wire was then glued with a droplet of paint to a copper extension wire (2 cm in length) which was inserted into the input of the EPG headstage amplifier. Another copper electrode (10 cm length, 2 mm diameter) was inserted into the soil of the plant container. Aphids were starved for *c.* 1 h as an adaptation period between the time of wiring and the beginning of EPG recording. Aphids were then placed on the abaxial side of the leaf. Plant, aphid and amplifier were placed in a Faraday cage to avoid noise. Waveform patterns were scored according to the categories described by Tjallingii & Hogen-Esch (1993): nonpenetration (NP); pathway phase, penetrating between cells en route to the vascular tissue (C waveform); short intracellular punctures in epidermal or mesophyll cells (pd waveform); repetitive potential drops (R-pd waveform); salivary secretion into sieve elements (E1 waveform); phloem ingestion (E2 waveform); derailed stylets (F waveform); and xylem ingestion (G waveform). To analyze the effects of elevated CO_2 and R gene-mediated resistance on aphid feeding behaviour, a set of EPG variables were calculated as described by Backus *et al.* (2007): the total duration spent in pathway phase activities; the total duration spent in short intracellular punctures; the total duration spent in salivation; the total duration spent in phloem ingestion; number of short intracellular punctures before first salivation; total repetitive potential drop numbers; time to first salivation; and time to first phloem ingestion.

Plant iTRAQ proteomic analysis

Total proteins were extracted using the cold acetone method according to Qin *et al.* (2013). A 100 μl protein sample was

combined with an equal volume of tetraethylammonium bicarbonate (TEAB). The proteins in TEAB were digested with trypsin (3.3 μg of trypsin per 100 μg of total protein) at 37°C for 24 h, and the solvent was removed. Matrix-assisted laser desorption ionization-time of flight (MALDI TOF)/TOF analysis was conducted to test digestion efficiency. The iTRAQ labelling was performed according to the manual procedure provided in the iTRAQ labelling kit (Applied Biosystems, Foster City, CA, USA). The iTRAQ-labelled samples were then pooled and subjected to strong cation exchange (SCX) fractionation using a high-performance liquid chromatography (HPLC) system (Shimadzu, Kyoto, Japan) connected to an SCX column (Luna 5 μm column, 4.6 mm i.d. × 250 mm, 5 μm, 100 Å; Phenomenex, Torrance, CA, USA) according to Qin *et al.* (2013). The eluted fractions were dried in a vacuum concentrator and then dissolved with 0.1% formic acid before reversed-phase nLC-tandem MS.

Peptide and protein identifications were performed with the ProteinPilo Software 4.0.8085 revision 148085 (AB SCIEX, Warrington, UK) using the Paragon algorithm. Combined data and spectra from each off-gel electrophoresis (OGE) fraction were searched against the NCBI database and a genome database of *M. truncatula* (http://www.medicagogenome.org). Proteins with significant changes in abundance upon aphid infestation with different treatments were selected using a method described by Abdallah *et al.* (2012). Protein ratios outside this range were defined as being significantly different at $P = 0.05$. The cutoff value for the down-regulated proteins was 0.8-fold and for the up-regulated proteins was 1.2-fold. To analyze the network of plant defensive signaling pathways in *M. truncatula*, the annotated proteins were mapped to the KEGG (Kyoto Encyclopedia of Genes and Genomes) metabolic pathways (http://www.genome.jp/kegg/pathway.html). Proteins associated with the plant defense were used to analyze these defensive pathway responses to aphid infestation. A heat map and a diagram were created. In the heat map, up-regulated proteins are red, and down-regulated proteins are shown in blue. The color saturation is proportional to the fold-changes (Fig. 5).

Gene expression

The RNA Easy Mini Kit (Qiagen, Valencia, CA, USA) was used to isolate total RNA from *M. truncatula* leaves, and 1 μg of RNA was used to synthesize cDNAs. mRNAs of the following target genes involved in the plant defense signaling pathway were quantified by real-time quantitative PCR: the membrane receptor somatic embryogenesis receptor kinase (SERK); calcium-dependent protein kinase (CDPK) in the calcium signaling pathway; mitogen-activated protein kinase kinase kinase 1 (MEKK1) in the MAPK signaling pathway; BGL and PR1 in the SA signaling pathway; allene oxide synthase (AOS) and 12-oxophytodienoate reductase protein (OPR) in the JA signaling pathway; GST and POD in the ROS pathway; HSP90, suppressor of the G2 allele of SKP1 (SGT), and required for Mla12 resistance 1 (RAR1) in ETI defenses; and SCF ubiquitin ligase (SKP1) in the ubiquitin-mediated proteolysis (UMP) signaling pathway. Specific primers for the genes were designed from the *M. truncatula* expressed sequence tags using Primer5 software (Supporting Information Table S1). The housekeeping gene β-actin was used as the internal quantitative PCR (qPCR) standard to analyze plant gene expression. The fold-changes of the target genes were calculated using the $2^{-\Delta\Delta Ct}$ normalization method. Each combination of aphid infestation, plant genotype and CO_2 concentration was represented by four biological replicates, and each biological replicate contained four technical repeats.

HSP90 gene silencing in Jester

The open reading frame fragments HSP90 (MTR_1g099840) and PDS (as a marker gene to confirm that the vector was available) of *M. truncatula* were obtained from the cDNA of the total RNA extracted from A17 leaves by PCR using primers (HSP-F: CGGGATCCAGGAAGTGGACGATTCCTTC; HSP-R: CGAGCTCCCAAATCCTCCTTTGTCATAC; PDS-F: CGGGATCCATGTCAGTAACTTGTAAGGAATAG; PDS-R: CGAGCTCTCAAAATTTAATATTTCTTGC). The HSP90 and PDS fragments were inserted into the *Bam*HI and *Sac*I sites of modified vector pGreenII via the virus-induced gene silencing (VIGS) method (Hellens *et al.*, 2000), in which a 35S promoter was inserted into *Apa*I and *Xho*I sites. The two recombinant plasmids, named pGreenPDS and pGreenHSP, were then transformed into *Agrobacterium tumefaciens* strain GV3101. About 0.2 ml of *A. tumefaciens* culture ($OD_{600} = 0.6$) with or without the vector was infiltrated into the fourth mature trifoliate leaf from the base of the shoot of each 6-wk-old normal Jester plant to get HSP90-silenced plants (confirmed with the gene expression of target gene MTR_1g099840). Normal 6-wk-old Jester plants grown in OTCs were selected to be infiltrated with vector and, 10 d later, HSP90 was silenced. Twelve HSP90-silenced Jester plants and 12 empty-vector Jester plants were selected to determine how silencing of HSP90 affects *A. pisum* feeding behavior. Six HSP90-silenced Jester plants and six empty-vector Jester plants were selected; the second and third trifoliate leaves from the top of each plant were infested with 50 apterous 4^{th}-instar nymphs. Another six HSP90-silenced Jester plants and six empty-vector Jester plants were selected as uninfested control plants. At 24 h after infestation, RNA was extracted from the HSP90-silenced plants and control plants, and the gene expression of HSP90, AOS, OPR and SKP1 were determined by quantitative reverse transcriptase (qRT)-PCR as described before. In addition, the MRGR of aphids reared on HSP90-silenced and empty-vector Jester plants under both CO_2 concentrations was determined.

Statistical analyses

The main effects of CO_2, plant genotype and aphid infestation on plant gene expression were tested according to the model below (ANOVA, Pasw Statistics 18.0, SPSS Inc., Chicago, IL, USA). A split-split plot design was used with CO_2 and block (a pair of OTCs with ambient and elevated CO_2) as the main effects, *M. truncatula* genotype as the subplot effect and aphid infestation level as the sub-subplot effect:

$$X_{ijklm} = \mu + C_i + B(C)_{j(i)} + G_k + CG_{ik} + GB(C)_{kj(i)} + A_l + CA_{il} + AB(C)_{lj(i)} + GAB(C)_{klj(i)} + e_{m(ijkl)}$$

where C is the CO_2 treatment ($i = 2$), B is the block ($j = 4$), G is the *M. truncatula* genotype ($k = 2$), A is the aphid infestation treatment ($l = 2$) and $e_{m(ijkl)}$ represents the error (ANOVA, SAS Institute). Tukey's multiple range tests were used to separate means when ANOVAs were significant ($P < 0.05$). For quantifying plant growth traits, aphid feeding behavior and population numbers as affected by *M. truncatula* genotype and CO_2 concentration, a split-plot design was also applied, with CO_2 and block as the main effects and *M. truncatula* genotype as the subplot effect. The chi-square test was used to analyze data derived from choice tests. All data were checked for normality and equality of residual error variances and were transformed (log or square-root) if needed to satisfy the assumptions of the analysis of variance.

Results

Plant growth traits

In the absence of aphid infestation, elevated CO_2 increased the photosynthetic rate by 45.4 and 48.6%, Chl content by 10.8 and 13.3%, biomass by 42.7 and 56.7%, and pod number by 29.4 and 34.2% for A17 and Jester, respectively (Fig. 1). Elevated CO_2 did not affect the flowering time or flower number of either genotype. Regardless of CO_2 concentration, the photosynthetic rate, Chl content, biomass, pod number, flower number and time

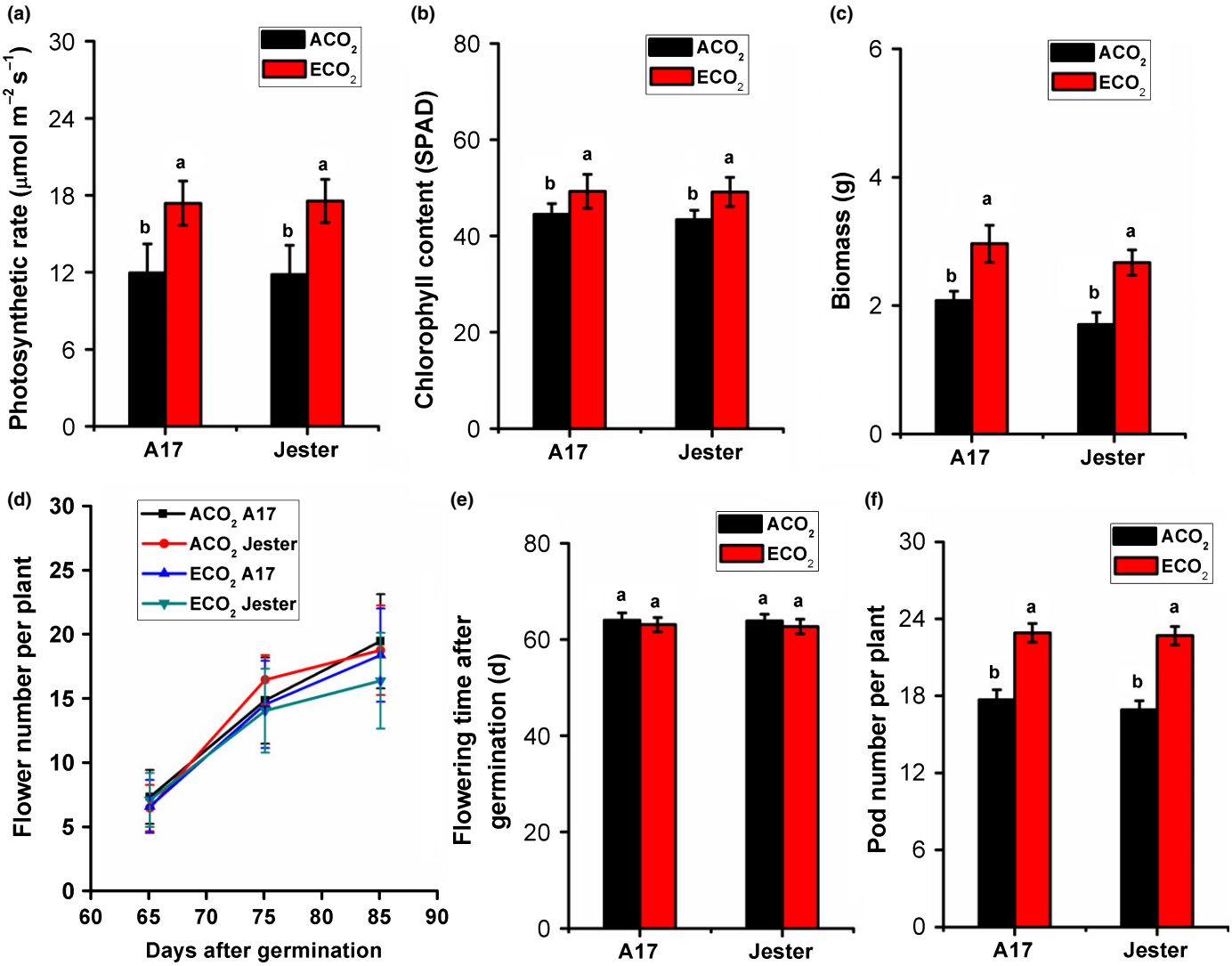

Fig. 1 Growth traits of two *Medicago truncatula* genotypes (A17 and Jester) grown under ambient CO_2 (ACO_2) and elevated CO_2 (ECO_2) without aphid infestation. (a) Photosynthetic rate, (b) Chl content, (c) biomass, (d) flower number per plant, (e) flowering time and (f) pod number per plant. Each value represents the mean (±SE) of four replicates. Different lowercase letters indicate significant differences between ACO_2 and ECO_2 within the same genotype plant as determined by Tukey's multiple range test at $P < 0.05$. There was no significant difference between A17 and Jester plants within the same CO_2 treatment.

of first flowering did not significantly differ between the two *M. truncatula* genotypes (Fig. 1).

Aphid abundance

Elevated CO_2 increased *A. pisum* abundance on A17 plants but decreased *A. pisum* abundance on Jester plants (Fig. 2a). Under ambient CO_2, *A. pisum* abundance was greater on A17 than on Jester, and this difference was greatly increased under elevated CO_2 (Fig. 2a).

Elevated CO_2 increased *A. pisum* MRGR on A17 plants but decreased *A. pisum* MRGR on Jester plants (Fig. 2b). Aphid MRGR was higher on A17 than on Jester plants regardless of CO_2 concentration (Fig. 2b). In the choice test, *A. pisum* preferred A17 plants to Jester plants regardless of CO_2 concentration (Fig. 2c).

Aphid feeding behavior

The total time that *A. pisum* spent in the pathway phase, penetrating between cells en route to the vascular tissue (C wave), was unaffected by elevated CO_2 and also did not differ significantly between A17 and Jester plants (Fig. 3a). Elevated CO_2 increased the total time of intracellular punctures in epidermal or mesophyll cells on A17 plants but did not significantly affect this parameter on Jester plants (Fig. 3b). Before the first salivation, elevated CO_2 increased the intracellular puncture numbers on A17 plants but decreased the intracellular puncture numbers on Jester plants, and intracellular puncture numbers before the first salivation were greater on A17 than on Jester plants (Fig. 3c).

Elevated CO_2 shortened the time to the first salivation and the time to phloem sap ingestion on A17 plants but tended to prolonged the time to first phloem ingestion on Jester plants (Fig. 3d,e). Under ambient CO_2, the time to the first phloem ingestion was greater on Jester plants than on A17 plants. Under elevated CO_2, the time to the first salivation and first phloem ingestion was greater on Jester plants than on A17 plants (Fig. 3d,e).

The repetitive potential drop waveform was a prerequisite for phloem feeding by *A. pisum*. Elevated CO_2 increased repetitive potential drop numbers on A17 plants but decreased them on Jester plants (Fig. 3f). Repetitive potential drop number was lower on Jester plants than on A17 plants regardless of CO_2 concentration (Fig. 3f).

Once the aphid stylet penetrated the phloem, elevated CO_2 shortened the salivation time and prolonged the phloem ingestion time on A17 plants, but the opposite was true on Jester plants (Fig. 3g,h). In addition, the total salivation time was shorter and phloem sap ingestion time was longer on A17 plants than on Jester plants. Phloem ingestion was not detected in aphids on Jester plants within the 8 h recording period (Fig. 3h).

iTRAQ-based proteomics analysis

Across all eight treatments (2 plant genotypes × 2 CO_2 levels × 2 levels of aphid infestation), a total of 1592 proteins were identified in the library uniprot_*Medicago truncatula*. These proteins are involved in a wide range of metabolic and signaling pathways (Fig. 4). Protein expression was considered to be up-regulated if the ratio of expression in aphid-infested plants/uninfested plants was > 1.2 and was considered to be down-regulated if the ratio

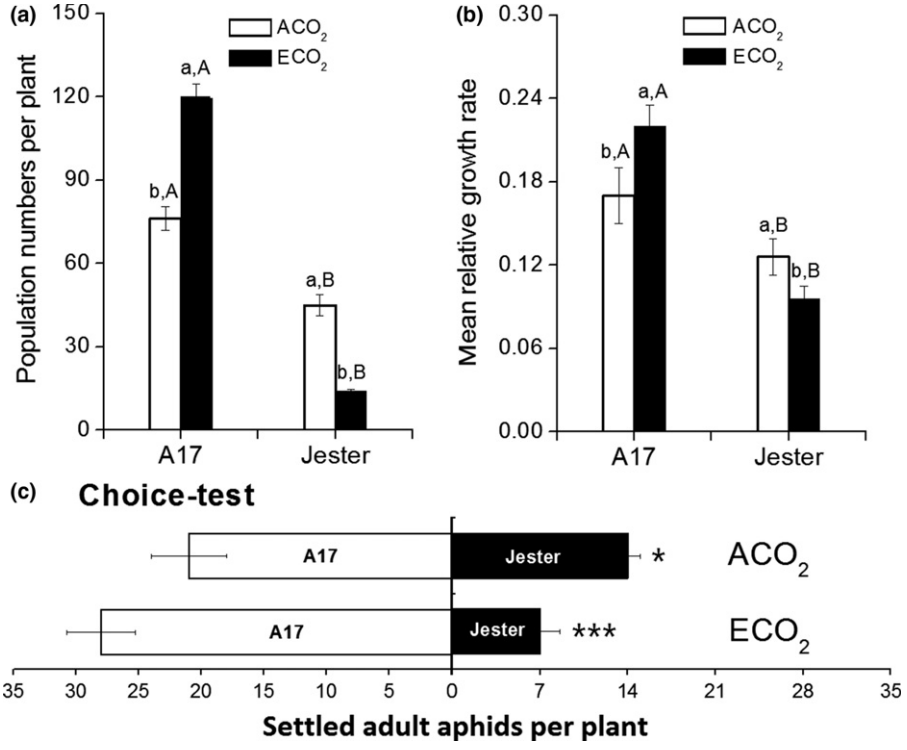

Fig. 2 *Acyrthosiphon pisum* performance on two *Medicago truncatula* genotypes (A17 and Jester) grown under ambient CO_2 (ACO_2) and elevated CO_2 (ECO_2). (a) *A. pisum* number per plant, (b) mean relative growth rate of *A. pisum* and (c) *A. pisum* choice between the two genotypes. For (a) and (b), each value represents the mean (± SE) of four replicates; different lowercase letters indicate significant differences between ACO_2 and ECO_2 within the same genotype plant, and different uppercase letters indicate significant differences between A17 and Jester plants within the same CO_2 treatment as determined by Tukey's multiple range test at $P < 0.05$. For (c), bars represent means ± SE; each test involved 16 replicates under ambient and elevated CO_2, and statistical significance between A17 and Jester plants under each CO_2 concentration is indicated: *, $P < 0.05$; ***, $P < 0.01$.

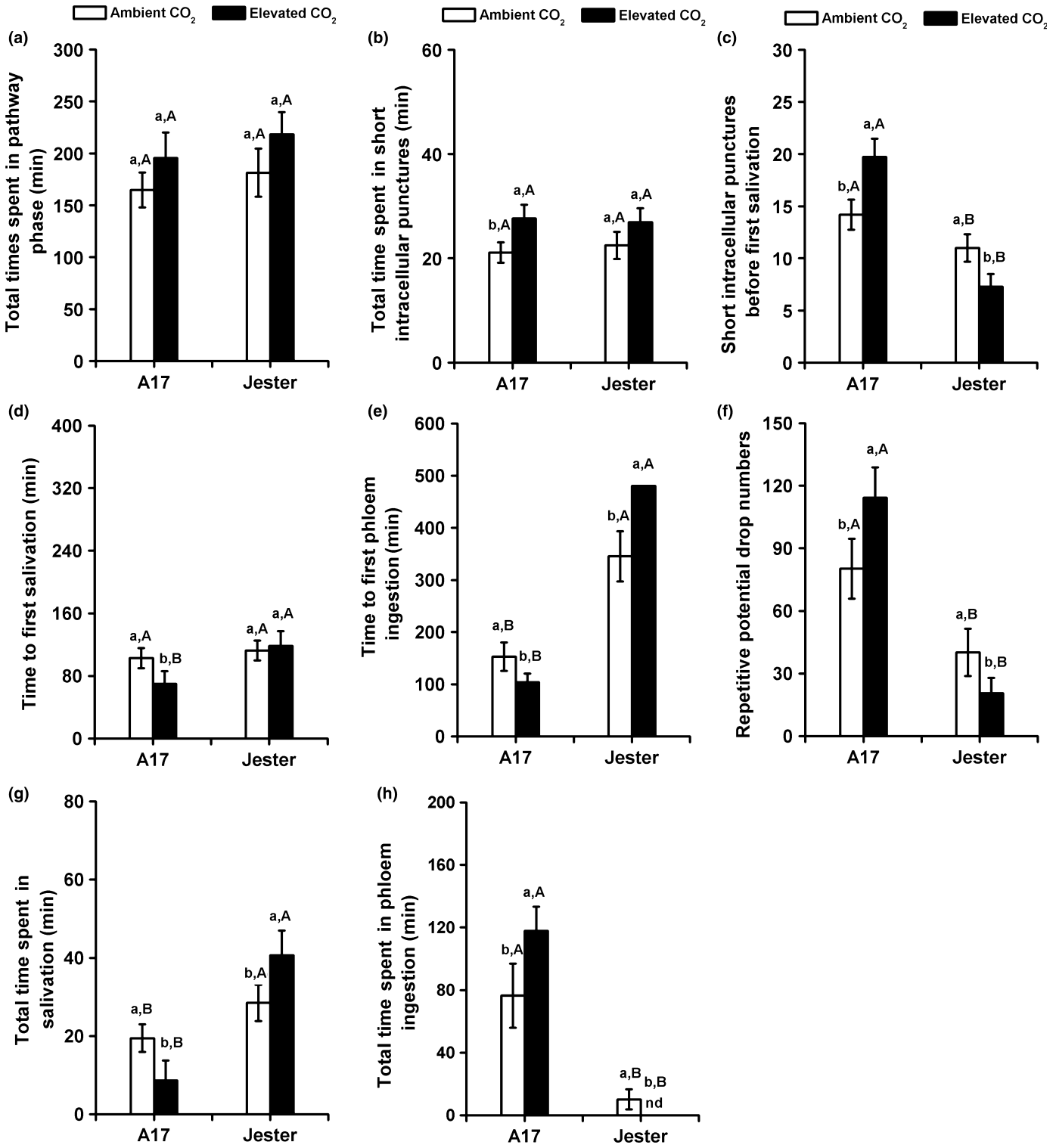

Fig. 3 Electrical penetration graph (EPG) results for *Acyrthosiphon pisum* feeding for 12 h on two *Medicago truncatula* genotypes (A17 and Jester) grown under ambient CO_2 and elevated CO_2. (a) Total time spent in pathway phase; (b) total time spent in short intracellular punctures; (c) short intracellular punctures before first salivation; (d) time to first salivation; (e) time to first phloem ingestion; (f) repetitive potential drop numbers; (g) total time spent in salivation; and (h) total time spent in phloem ingestion. Each value is the mean (± SE) of 24 biological replicates. Different lowercase letters indicate significant differences between CO_2 treatments within the same genotype. Different uppercase letters indicate significant differences between A17 and Jester plants within the same CO_2 treatment as determined by Tukey's multiple range test at $P < 0.05$. nd, not detectable.

was < 0.8 at $P < 0.05$ (Fig. 4a). For A17 plants under ambient CO_2, aphid infestation decreased the expression of 366 proteins but increased the expression of 411 proteins. For A17 plants under elevated CO_2, aphid infestation decreased the expression of 279 proteins but increased the expression of 305 proteins. For Jester plants under ambient CO_2, aphid infestation decreased the

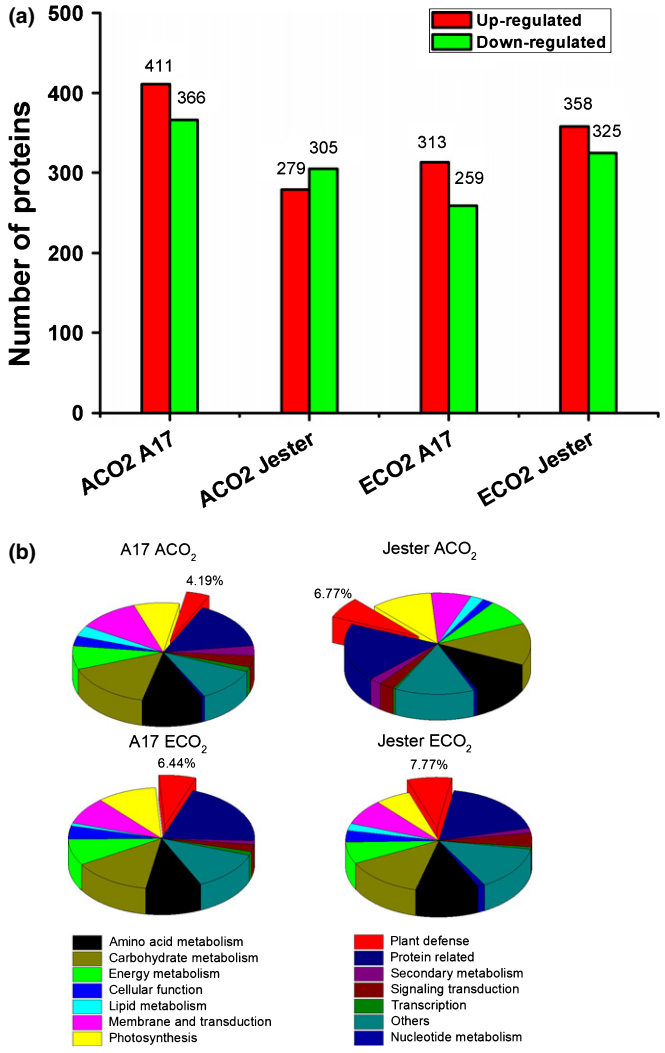

Fig. 4 Changes in protein profiles in response to *Acyrthosiphon pisum* infestation as affected by plant genotype of *Medicago truncatula* (A17 and Jester) and CO_2 concentration (ambient (ACO_2) and elevated (ECO_2)). (a) The number of up-regulated and down-regulated proteins. Protein expression was considered to be up-regulated or down-regulated if the expression was ≥ 1.2-fold greater ($P \leq 0.05$) or ≤ 0.8-fold smaller ($P \leq 0.05$), respectively, in aphid-infested than in noninfested plants. (b) Protein classification based on KEGG pathway analyses. The percentages of up-regulated proteins involved in plant defense are indicated.

expression of 313 proteins but increased the expression of 259 proteins. For Jester plants under elevated CO_2, aphid infestation decreased the expression of 358 proteins but increased the expression of 325 proteins. Those proteins that share homology with genes of known function in the database were categorized according to biological process (Fig. 4b). Aphid infestation-induced proteins included those involved in amino acid metabolism, carbohydrate metabolism, energy metabolism, cellular function, lipid metabolism, membrane and transduction, photosynthesis, plant defense (induced defensive signaling pathways after infestation by a pathogen or insect), protein-related, secondary metabolism (the biosynthesis and degradation of secondary metabolites including terpenoids, flavonoids and carotenoids), signal transduction (some signaling pathways demonstrating how ligands binding to their receptors can affect second messengers and eventually result in altered cellular responses, which exclude defensive signaling pathways), transcription and nucleotide metabolism. Among all proteins up-regulated in response to *A. pisum* infestation, the percentage involved in defense signaling was 4.19 and 6.77% in A17 plants under ambient CO_2 and elevated CO_2, respectively, and was 6.44 and 7.77% in Jester plants under ambient CO_2 and elevated CO_2, respectively (Fig. 4b).

Protein expression associated with plant defenses

The proteomics data indicated that *A. pisum* infestation induced defense-associated proteins in both genotypes under both CO_2 concentrations (Fig. 5). For A17 plants, *A. pisum* triggered defenses associated with PTI rather than ETI due to the lack of an R gene. In A17 plants, 27 and 25 proteins related to PTI defenses were up-regulated by aphids under ambient CO_2 and elevated CO_2, respectively. These up-regulated PTI defenses included the MAPK signaling pathway, Ca^{2+} signaling, ROS-related antioxidase enzymes and the SA signaling pathway. In A17 plants, however, *A. pisum* infestation suppressed four proteins involved in the JA signaling pathway under ambient CO_2 and suppressed four other proteins under elevated CO_2.

For Jester plants, aphid infestation not only triggered PTI defenses (including the MAPK signaling pathway, ROS-related antioxidase enzymes and the SA signaling pathway) but also activated a series of HSP genes, JA signaling pathways and UMP under both CO_2 concentrations, which suggested that up-regulation of HSP, JA signaling pathways and UMP is characteristic of ETI defenses (Fig. 5). In Jester plants, *A. pisum* infestation up-regulated 14 proteins and down-regulated four proteins involved in PTI under ambient CO_2 and up-regulated 12 proteins and down-regulated 11 proteins involved in PTI under elevated CO_2. Aphid infestation of Jester plants also up-regulated 10 proteins involved in ETI under ambient CO_2 and up-regulated 12 proteins involved in ETI under elevated CO_2.

Expression of defense genes

To confirm the results of iTRAQ-based proteomics and to determine the effect of elevated CO_2 on aphid infestation-induced defenses in *M. truncatula* plants, we quantified expression of key genes involved in PTI (including the early signaling kinases SERK, CDPK and MEKK1; the SA signaling pathway-regulated genes PR and BGL; and the ROS-related antioxidases POD and SOD), and of key genes involved in ETI (including the HSP90 genes MTR_1g099840, MTR_5g097320 and MTR_1g025430; the co-chaperones RAR1 and SGT1; the JA signaling pathway-regulated genes AOS and OPR; and the UMP-related gene SKP1) in both plant genotypes (Figs 6–8).

A comparison of uninfested vs infested plants showed that aphid infestation up-regulated the expression of PTI-related genes in A17 plants regardless of CO_2 concentration. In Jester plants, aphid infestation up-regulated the SA signaling pathway and antioxidases regardless of CO_2 concentration and up-regulated MEKK1 under ambient CO_2 (Figs 6a–c, 8a–d; Tables

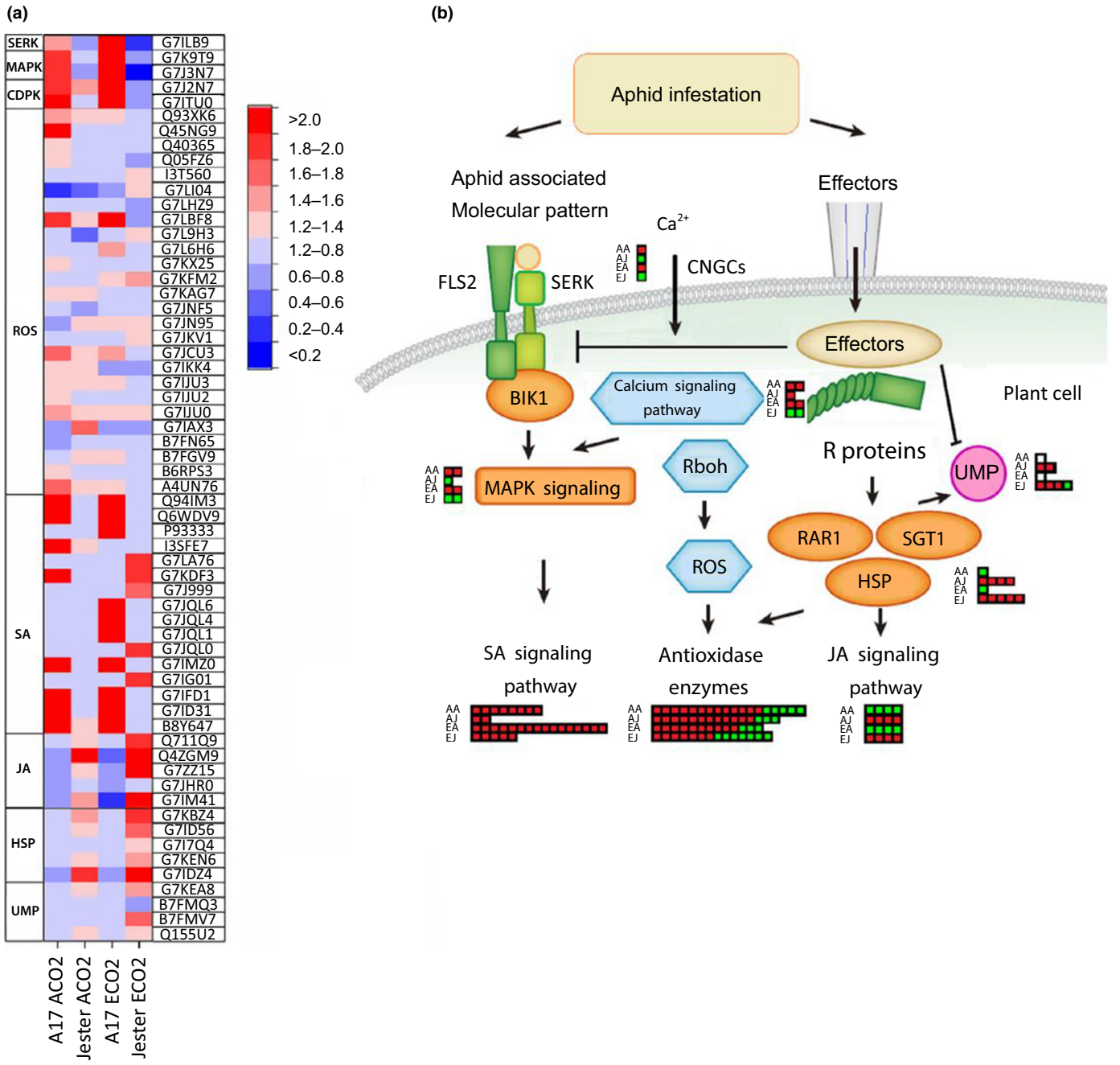

Fig. 5 Cluster analysis (a) and the diagram (b) of aphid infestation-induced defense-related proteins in two *Medicago truncatula* genotypes (A17 and Jester) under both CO_2 concentrations (ambient (ACO_2) and elevated (ECO_2)) according to proteomics data. The induced enzymes and pathways included the kinases somatic embryogenesis receptor-like kinase (SERK), mitogen-activated protein kinase (MAPK) and calmodulin-like domain protein kinase (CDPK); reactive oxygen species-related antioxidase enzymes (ROS); the salicylic acid signaling pathway (SA); the jasmonic acid signaling pathway (JA); HSP90 and its co-chaperone (HSP); and ubiquitin-mediated proteolysis (UMP). In the diagram, the red and green squares represent the numbers of up-regulated (> 1.2-fold) and down-regulated proteins (< 0.8-fold) of aphid infestation, respectively, in each pathway. AA, A17 under ambient CO_2; AJ, Jester under ambient CO_2; EA, A17 under elevated CO_2; EJ, Jester under elevated CO_2; FLS2, Flagellin-sensing 2; CNGCs, cyclic nucleotide-gated channels; BIK1, botrytis-induced kinase 1; Rboh, respiratory burst oxidase homologs.

S2–S5). Elevated CO_2 up-regulated the expression of PTI-related genes including those that encode the kinases SERK, CDPK and MEKK1, as well as PR and BGL of the SA signaling pathway in aphid-infested A17 plants (Figs 6a–c, 8a,b). By contrast, elevated CO_2 up-regulated the SA signaling pathway but down-regulated the expression of CDPK and MEKK1 in aphid-infested Jester plants (Figs 6a–c, 8a,b). The expression of SERK, CDPK, MEKK1, PR1 and BGL was higher in aphid-infested A17 plants than in aphid-infested Jester plants regardless of CO_2 concentration (Figs 6a–c, 8a,b).

Regardless of CO_2 concentration, the expression of the following ETI-related genes was up-regulated in response to aphid

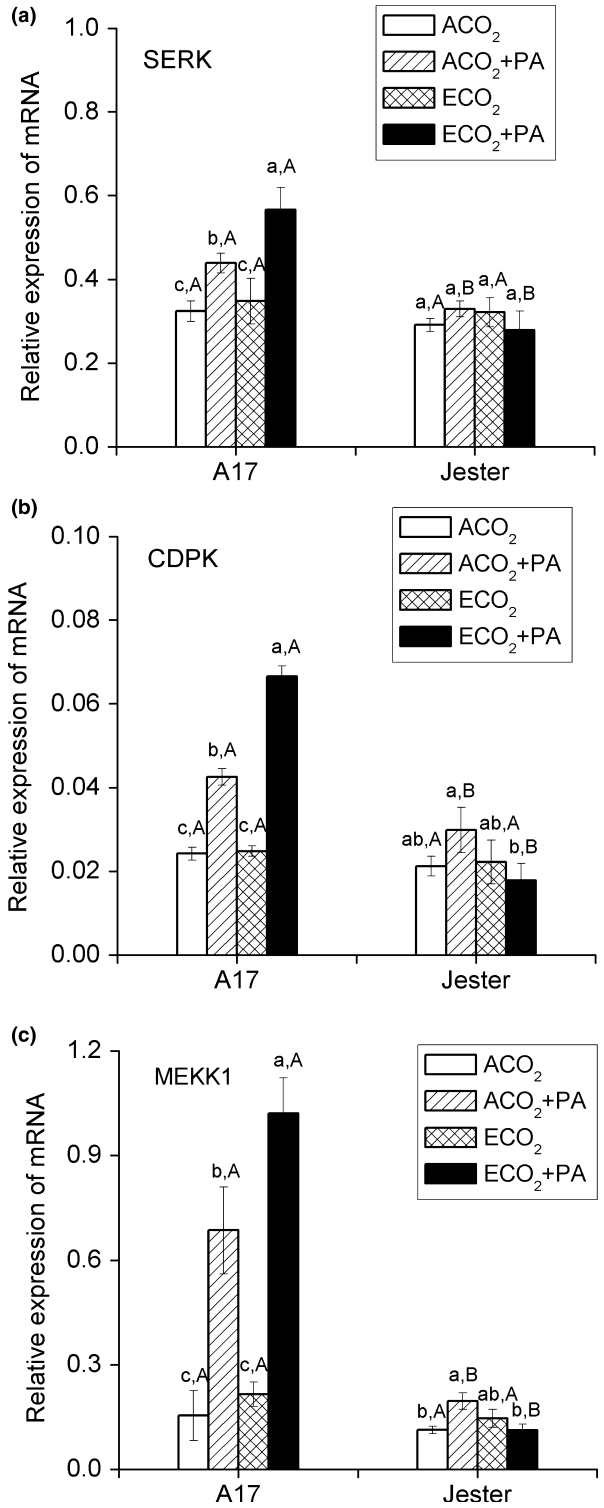

Fig. 6 Expression of early plant kinases involved in PAMP-triggered immunity (PTI) of two *Medicago truncatula* genotypes grown under ambient CO_2 (ACO_2) and elevated CO_2 (ECO_2) with and without pea aphid (PA) infestation. (a) SERK, (b) CDPK and (c) MEKK1. Each value is the mean (± SE) of four replicates. Different lowercase letters indicate significant differences among the combinations of aphid treatment and CO_2 concentration within the same genotype. Different uppercase letters indicate significant differences between genotypes within the same CO_2 concentration and aphid treatment as determined by Tukey's multiple range test at $P < 0.05$.

infestation in Jester plants but not in A17 plants: the three HSP90 genes; the co-chaperones SGT1 and RAR1; AOS and OPR in the JA signaling pathway; and the UMP-related SKP1 (Figs 7, 8e–g). Furthermore, elevated CO_2 increased the expression of ETI defenses of aphid-infested Jester plants but not of aphid-infested A17 plants (Figs 7, 8e–g). Expression of the following genes was higher in aphid-infested Jester plants than in aphid-infested A17 plants: the three HSP90 genes and their co-chaperones SGT1 and RAR1; AOS and OPR in the JA signaling pathway; and SKP1 in UMP.

Gene expression and aphid performance on HSP90-VIGS Jester plants

When the HSP90 (MTR_1g099840) gene was artificially silenced in Jester, the expression of genes involved in ETI was reduced in response to aphid infestation, that is, expression of AOS and OPR in the JA signaling pathway and SKP1 in UMP was lower in HSP90-silenced than in normal Jester plants (Fig. 9b–d). Furthermore, pea aphids reared on HSP90-deficient Jester plants showed decreased salivation and increased phloem ingestion time and spent less time reaching the E2 wave than pea aphids reared on normal Jester plants (Fig. 9e–f). These results suggested that HSP90 deficiency impaired JA resistance and UMP in Jester plants and consequently enhanced the feeding efficiency of pea aphids. Furthermore, elevated CO_2 did not affect the MRGR of aphids reared on HSP90-deficient Jester plants, suggesting that the negative effect of elevated CO_2 on aphid performance on normal Jester plants (see Fig. 2) results from the enhancement of HSP90 and ETI signaling (Fig. 9g). Thus, the CO_2-induced up-regulation of HSP90 and ETI defenses is responsible for the decrease in aphid MRGR in Jester plants under elevated CO_2.

Discussion

Previous transcriptomic studies have shown that elevated CO_2 affects various signaling pathways in C_3 plants, including photosynthesis, development, defense and nutrition; these changes in signaling pathways then alter the performance of herbivorous insects (Casteel *et al.*, 2008; Sun *et al.*, 2013). The proteomics results of the current report showed that the response to the aphid *A. pisum* differed greatly between an aphid-resistant genotype of *M. truncatula* (Jester, which has the R gene APR) and a susceptible genotype (A17, which lacks the R gene APR) under elevated CO_2, and that this difference resulted from differences in the expression of genes in defensive signaling pathways under elevated CO_2. For susceptible A17 plants, elevated CO_2 increased PTI defenses including the MAPK signaling pathway, Ca^{2+} signaling pathways and the SA signaling pathway, but decreased the JA signaling pathway. As a consequence, elevated CO_2 improved the performance of the aphid on A17 plants. For resistant Jester plants, by contrast, elevated CO_2 decreased PTI defenses but increased ETI defenses. As a consequence, elevated CO_2 decreased the performance of the aphid on Jester plants. A VIGS experiment further showed that silencing of HSP90 in Jester

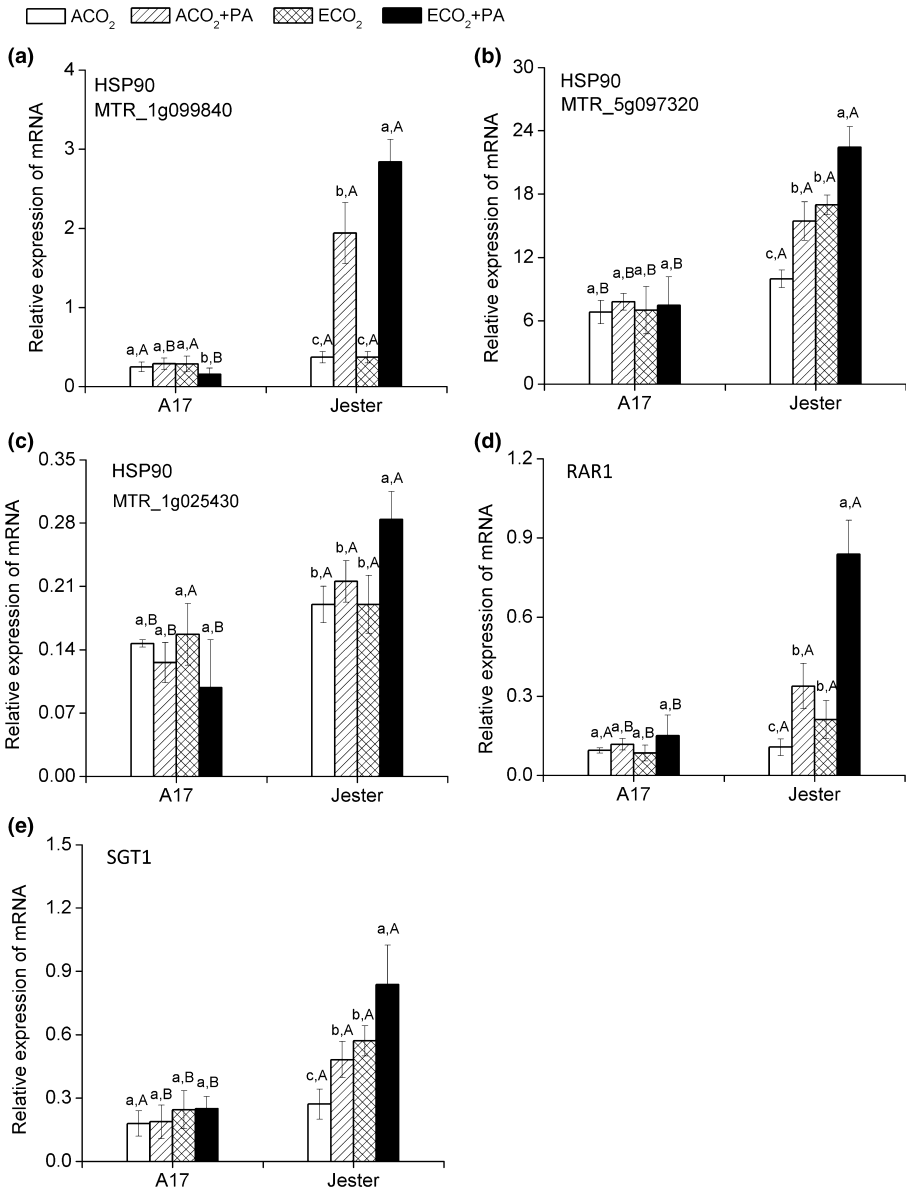

Fig. 7 Expression of three HSP90 genes and their co-chaperones (RAR1 and SGT1), which are involved in effector-triggered immunity (ETI), in two *Medicago truncatula* genotypes (A17 and Jester) grown under ambient CO_2 (ACO_2) and elevated CO_2 (ECO_2) with and without pea aphid (PA) infestation. (a) HSP90 (MTR_1g099840), (b) HSP90 (MTR_5g097320), (c) HSP90 (MTR_1g025430), (d) RAR1 and (e) SGT1. Each value is the mean (± SE) of four replicates. Different lowercase letters indicate significant differences among the combinations of aphid treatment and CO_2 concentration within the same genotype. Different uppercase letters indicate significant differences between genotypes within the same CO_2 concentration and aphid treatment as determined by Tukey's multiple range test at $P < 0.05$.

plants impaired ETI signaling and the JA signaling pathway and nullified the plant-mediated negative effects of elevated CO_2 on aphid performance. These results indicate that 'the impairment of efficient resistance hypothesis' may explain why elevated CO_2 improves the performance of aphids on plants that rely on PTI (on plants that lack an R gene against aphids) but obviously does not explain why elevated CO_2 reduces the performance of aphids on plants that rely on ETI (on plants that have an R gene against aphids). To our knowledge, this is the first report to provide a molecular explanation for why elevated CO_2 may reduce rather than enhance the performance of aphids on plants with R genes.

R gene-dependent resistance is an efficient form of defense against target insects because it is not activated unless the plant is attacked, that is, until the plant recognizes specific salivary effectors from the target insect (Hogenhout & Bos, 2011). In comparison, resistance based on pre-formed phytohormones and other compounds requires more resources because the basal defenses are maintained even when the plant is not being attacked. For example, glucosinolate-dominant plant genotypes invested more resources into glucosinolate synthesis and less resources into growth than wild-type plants under elevated CO_2 (Gabriela Bidart-Bouzat, 2004; Vannette & Hunter, 2011). The current results indicated that the fitness of the resistant genotype of *M. truncatula* was not reduced in the absence of aphids, that is, the resistant and susceptible genotypes had similar growth traits regardless of CO_2 concentration. Thus, the growth and yield of Jester plants would not be reduced relative to the growth and yield of A17 plants in the absence of aphid infestation or in the presence of elevated CO_2.

Although elevated CO_2 increased the growth and biomass of both A17 and Jester plants, the effects of elevated CO_2 on aphid abundance and MRGR differed between the plant genotypes. In addition, the feeding behavior and real-time stylet locations of aphids indicated that the effects of elevated CO_2 on plant

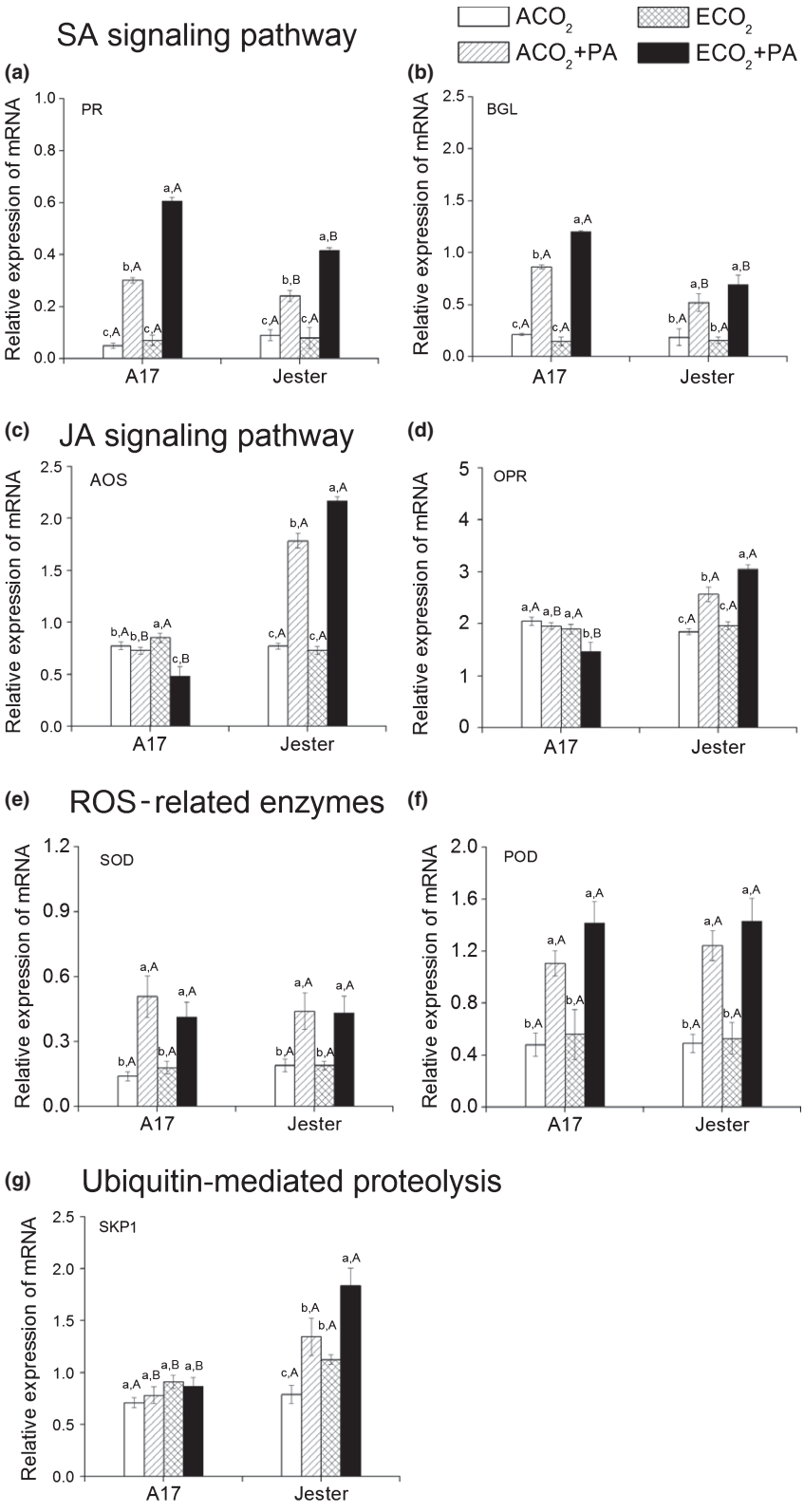

Fig. 8 Expression of defensive genes of two *Medicago truncatula* genotypes (A17 and Jester) grown under ambient CO_2 (ACO_2) and elevated CO_2 (ECO_2) with and without pea aphid (PA) infestation. (a) PR and (b) BGL in the salicylic acid (SA) signaling pathway; (c) AOS and (d) OPR in the jasmonic acid (JA) signaling pathway; (e) SOD and (f) POD related to reactive oxygen species (ROS); and (g) SKP1 in the ubiquitin-mediated proteolysis (UMP) signaling pathway. Each value is the mean (± SE) of four replicates. Different lowercase letters indicate significant differences among the combinations of aphid treatment and CO_2 concentration within the same genotype. Different uppercase letters indicate significant differences between genotypes within the same CO_2 concentration and aphid treatment as determined by Tukey's multiple range test at $P < 0.05$.

resistance in the mesophyll and phloem differed between genotypes. Specifically, the time spent probing before phloem ingestion under elevated CO_2 was greater on A17 plants than on Jester plants, indicating that elevated CO_2 increased the mesophyll resistance of A17 plants but decreased the mesophyll resistance of Jester plants. Once its stylet reached the phloem, *A. pisum* spent less time salivating and more time ingesting on A17 plants than on Jester plants under elevated CO_2, suggesting that elevated CO_2 decreased the phloem resistance of A17 but increased the phloem resistance of Jester. Evidence from plant–

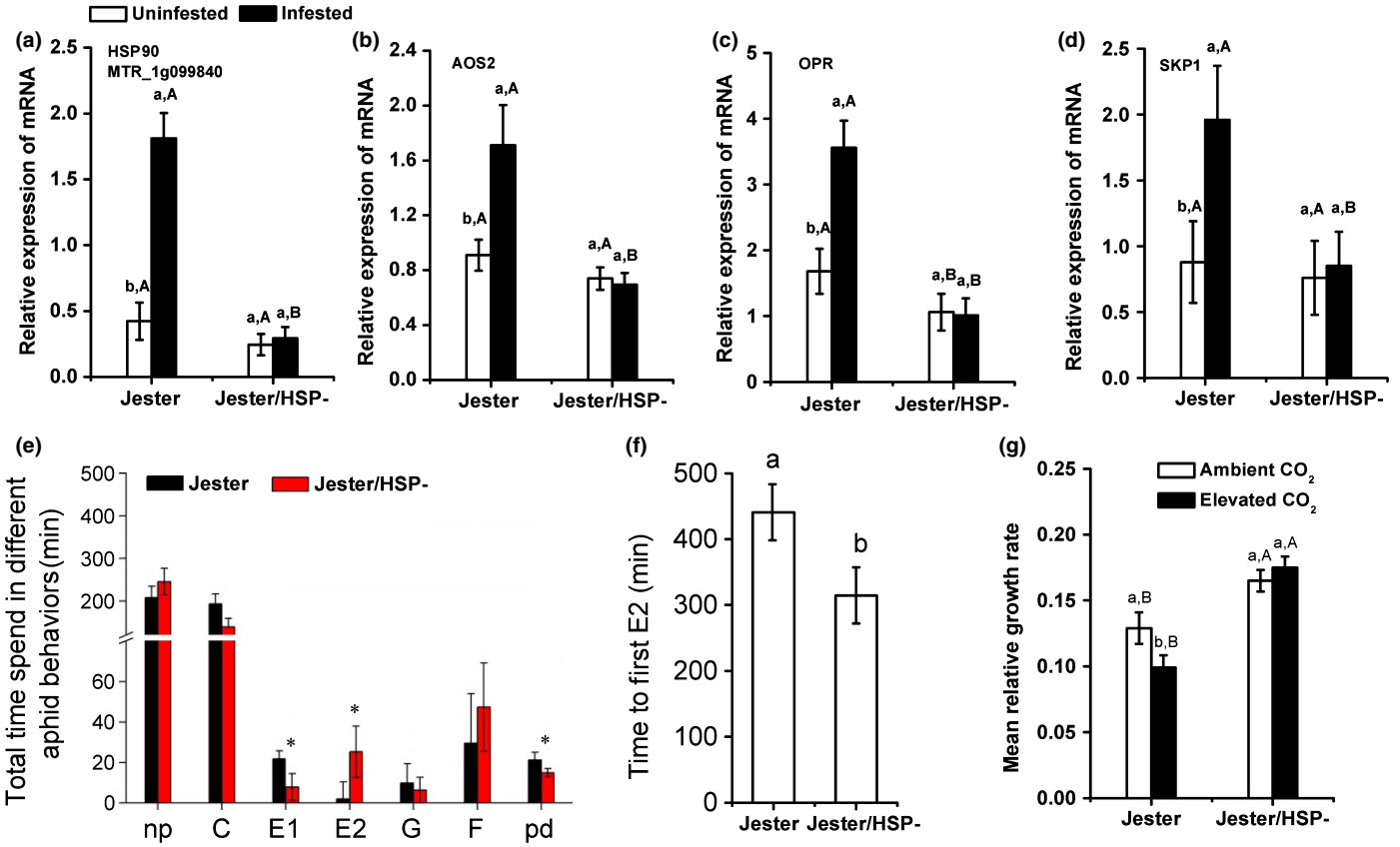

Fig. 9 Expression of HSP90 (MTR_1g099840) and defensive genes in the jasmonic acid (JA) and ubiquitin-mediated proteolysis (UMP) signaling pathways of HSP90-deficient (Jester/HSP-) and nondeficient Jester (Jester) plants of *Medicago truncatula* with and without pea aphid infestation (a–d), plus electrical penetration graph results for pea aphids feeding for 12 h on HSP90-deficient and nondeficient Jester plants grown under ambient CO_2 (e–f), and mean relative growth rate of aphids on HSP90-deficient and nondeficient Jester plants grown under ambient CO_2 and elevated CO_2 (g). For (a–d), each value is the mean (± SE) of six replicates; different lowercase letters indicate significant differences between aphid infestation and uninfestation treatments within the same genotype plants; and different uppercase letters indicate significant differences between HSP90-deficient Jester and normal Jester plants within the same aphid treatments as determined by Tukey's multiple range test at $P < 0.05$. (e) Statistical significance between plants of two genotypes under each CO_2 concentration is indicated by asterisks, each value is the mean (± SE) of 12 replicates. (f) Different lowercase letters indicate significant differences between two genotypes; each value is the mean (± SE) of 12 replicates. (g) Each value is the mean (± SE) of four replicates; different lowercase letters indicate significant differences between two CO_2 levels within the same genotype plants;, and different uppercase letters indicate significant differences between genotypes with the same CO_2 treatment as determined by Tukey's multiple range test at $P < 0.05$.

pathogen interactions showed that plant PTI defenses are mainly located in mesophyll cells and that single dominant R gene-dependent ETI defenses are phloem-specific (Kaloshian *et al.*, 1998; Klingler *et al.*, 1998; Bittel & Robatzek, 2007; Feng *et al.*, 2012). Our results suggest that R gene-dependent resistance against *A. pisum* in Jester is located in the phloem (i.e. it reduces phloem ingestion by the aphid) and that elevated CO_2 enhances the phloem resistance against the aphid in Jester by promoting ETI signaling.

PTI defenses against aphids are immediately initiated when the host plant is infested by aphids (Jaouannet *et al.*, 2014). Like pathogen elicitors, small molecules from insect saliva may be recognized by the membrane pattern recognition receptor BAK1/SERK, and such recognition may activate downstream defensive signaling pathways in host plants (Chaudhary *et al.*, 2014). According to the current proteomics and gene expression data, aphid infestation caused SERK in *M. truncatula* to stimulate typical PTI defenses in A17 plants. For the R gene-containing Jester, however, aphid infestation did not trigger SERK, and PTI defenses were lower in aphid-infested Jester plants than in aphid-infested A17 plants. Furthermore, elevated CO_2 increased PTI defenses (including the expression of defensive kinases SERK, CDPK and MEKK1) in A17 plants but decreased the expression of CDPK and MEKK1 in Jester plants, suggesting that elevated CO_2 increased mesophyll-located PTI defenses in A17 but decreased those defenses in Jester plants. According to previous studies, aphids are able to overcome mesophyll-located PTI defenses by secreting salivary effectors that suppress more effective host defenses (Zhu-Salzman *et al.*, 2004; Mewis *et al.*, 2005). Substantial evidence shows that the SA signaling pathway, a typical PTI defense against aphid infestation, has an antagonistic relationship with the JA signaling pathway, that is, an increase in PTI defense often results in a decrease in efficient defense. Our results also suggest that aphid performance under elevated CO_2 cannot be explained by the effects of aphids on PTI defenses in either genotype.

Several studies of aphid–plant interactions have indicated that ETI defense based on a single dominant R gene is phloem-specific, that is, involves inhibition of phloem feeding (Kaloshian *et al.*, 1998; Klingler *et al.*, 1998; Bittel & Robatzek, 2007; Feng *et al.*, 2012). For example, the R gene *Bph14* in rice plants can induce callose deposition in phloem cells and trypsin inhibitor production after planthopper infestation, which reduced the growth rate and longevity of the planthopper (Du *et al.*, 2009). In plant–pathogen interactions, pathogens trigger ETI defenses (including plant cell death, ROS and the JA signaling pathway) that suppress infection severity (Tsuda & Katagiri, 2010; Cui *et al.*, 2015). In the current study, aphid infestation up-regulated the JA signaling pathway in the genotype with the R gene (Jester) but not in the genotype without the R gene (A17), suggesting that the JA signaling pathway was important for ETI against aphids in the Jester genotype. Our results are consistent with a previous study that found that the JA signaling pathway is involved in AKR gene-dependent resistance in Jester against *A. kondoi* (Gao *et al.*, 2007). Furthermore, previous loss-of-function experiments showed that the JA signaling pathway provides effective resistance against aphids (Ellis *et al.*, 2002; Mewis *et al.*, 2006). Our results also suggest that differences in the activation of the JA signaling pathway help to explain differences in aphid performance on the Jester and A17 genotypes of *M. truncatula*. Elevated CO_2 enhanced the JA signaling pathway in Jester plants but decreased the JA signaling pathway in A17 plants, suggesting that plants with and without an R gene for aphid resistance will respond differently to elevated CO_2.

HSP90 and its chaperone complex are required for maintaining the stability of the R protein and for triggering downstream ETI defenses (Fu & Dong, 2013). The chaperone complex can also directly regulate the JA signaling pathway by either securing the steady-state levels of the receptor COI1 or by regulating the activity of E3 ubiquitin ligase SKP1 to enhance ubiquitin-mediated proteolysis (Azevedo *et al.*, 2002; Zhang *et al.*, 2008; Liu *et al.*, 2011; Wang *et al.*, 2016). Thus, our experiments showed that once the HSP90 (MTR_1g099840) gene was silenced in Jester, the JA signaling pathway and UMP were down-regulated, which enabled improved feeding by the target aphid. In addition, elevated CO_2 did not decrease the MRGR of aphids associated with HSP90-silenced Jester plants but did so on nonsilenced Jester plants. These results suggest that the up-regulation of HSP90 and co-chaperone proteins in Jester plants under elevated CO_2 enhances JA signaling and other ETI defenses and thereby reduces aphid fitness on Jester plants.

In summary, the current study found that increases in the R gene-related HSP90 under elevated CO_2 enhances the defenses of *M. truncatula* plants against the pea aphid, *A. pisum*. For a near-isogenic genotype that lacked the R gene, however, elevated CO_2 reduced defenses against the aphid. This study has generated several significant findings. First, the feeding behavior data and proteomics data showed that susceptible A17 plants and resistant Jester plants had different resistance patterns in response to aphid infestation. Second, elevated CO_2 increased phloem-located ETI defenses in Jester, which decreased *A. pisum* fitness. Finally and perhaps most importantly, elevated CO_2 increased the expression in Jester plants of HSP90, which is a key protein connecting the R protein with the JA signaling pathway and with other downstream factors affecting resistance against *A. pisum*. Our results suggest that genotypes with the R gene may have enhanced resistance against *A. pisum* under elevated CO_2 and that this enhanced resistance does not come at the expense of reduced plant productivity. These results have important implications for the breeding of pest-resistant crop plants under climate change.

Acknowledgements

This project was supported by the Strategic Priority Research Program of the Chinese Academy of Sciences (no. XDB11050400) and the National Nature Science Fund of China (nos. 31500332 and 31770452). We thank Dr Wenhao Zhang and Dr Lingling Gao for helpful discussions and advice.

Author contributions

Y.S., H.G. and F.G. planned and designed the research. Y.S., H.G. and E.Y. performed experiments, conducted fieldwork and analysed the data. Y.S. and H.G. wrote the manuscript.

References

Abdallah C, Sergeant K, Guillier C, Dumas-Gaudot E, Leclercq CC, Renaut J. 2012. Optimization of iTRAQ labelling coupled to OFFGEL fractionation as a proteomic workflow to the analysis of microsomal proteins of *Medicago truncatula* roots. *Proteome Science* **10**: 37.

Ainsworth EA, Rogers A. 2007. The response of photosynthesis and stomatal conductance to rising [CO_2]: mechanisms and environmental interactions. *Plant, Cell & Environment* **30**: 258–270.

Azevedo C, Sadanandom A, Kitagawa K, Freialdenhoven A, Shirasu K, Schulze-Lefert P. 2002. The RAR1 interactor SGT1, an essential component of R gene-triggered disease resistance. *Science* **295**: 2073–2076.

Backus EA, Cline AR, Ellerseick MR, Serrano MS. 2007. *Lygus hesperus* (Hemiptera: Miridae) feeding on cotton: new methods and parameters for analysis of nonsequential electrical penetration graph data. *Annals of the Entomological Society of America* **100**: 296–310.

Bittel P, Robatzek S. 2007. Microbe-associated molecular patterns (MAMPs) probe plant immunity. *Current Opinion in Plant Biology* **10**: 335–341.

Casteel CL, O'Neill BF, Zavala JA, Bilgin DD, Berenbaum MR, DeLucia EH. 2008. Transcriptional profiling reveals elevated CO_2 and elevated O_3 alter resistance of soybean (*Glycine max*) to Japanese beetles (*Popillia japonica*). *Plant, Cell & Environment* **31**: 419–434.

Chaudhary R, Atamian HS, Shen Z, Briggs SP, Kaloshian I. 2014. GroEL from the endosymbiont *Buchnera aphidicola* betrays the aphid by triggering plant defense. *Proceedings of the National Academy of Sciences, USA* **111**: 8919–8924.

Chini A, Grant JJ, Seki M, Shinozaki K, Loake GJ. 2004. Drought tolerance established by enhanced expression of the CC–NBS–LRR gene, ADR1, requires salicylic acid, EDS1 and ABI1. *Plant Journal* **38**: 810–822.

Cui H, Tsuda K, Parker JE. 2015. Effector-triggered immunity: from pathogen perception to robust defense. *Annual Review of Plant Biology* **66**: 487–511.

Du B, Zhang W, Liu B, Hu J, Wei Z, Shi Z, He R, Zhu L, Chen R, Han B. 2009. Identification and characterization of Bph14, a gene conferring resistance to brown planthopper in rice. *Proceedings of the National Academy of Sciences, USA* **106**: 22163–22168.

Ellis C, Karafyllidis I, Wasternack C, Turner JG. 2002. The Arabidopsis mutant *cev1* links cell wall signaling to jasmonate and ethylene responses. *Plant Cell* **14**: 1557–1566.

Feng F, Yang F, Rong W, Wu X, Zhang J, Chen S, He C, Zhou J-M. 2012. A *Xanthomonas* uridine 5'-monophosphate transferase inhibits plant immune kinases. *Nature* **485**: 114–118.

Fu ZQ, Dong X. 2013. Systemic acquired resistance: turning local infection into global defense. *Annual Review of Plant Biology* **64**: 839–863.

Gabriela Bidart-Bouzat M. 2004. Herbivory modifies the lifetime fitness response of *Arabidopsis thaliana* to elevated CO_2. *Ecology* **85**: 297–303.

Gao L-L, Anderson JP, Klingler JP, Nair RM, Edwards OR, Singh KB. 2007. Involvement of the octadecanoid pathway in bluegreen aphid resistance in *Medicago truncatula*. *Molecular Plant-Microbe Interactions* **20**: 82–93.

Gao L-L, Klingler JP, Anderson JP, Edwards OR, Singh KB. 2008. Characterization of pea aphid resistance in *Medicago truncatula*. *Plant Physiology* **146**: 996–1009.

Guo H, Sun Y, Li Y, Liu X, Wang P, Zhu-Salzman K, Ge F. 2014a. Elevated CO_2 alters the feeding behaviour of the pea aphid by modifying the physical and chemical resistance of *Medicago truncatula*. *Plant, Cell & Environment* **37**: 2158–2168.

Guo H, Sun Y, Li Y, Liu X, Zhang W, Ge F. 2014b. Elevated CO_2 decreases the response of the ethylene signaling pathway in *Medicago truncatula* and increases the abundance of the pea aphid. *New Phytologist* **201**: 279–291.

Guo H, Sun Y, Li Y, Tong B, Harris M, Zhu-Salzman K, Ge F. 2013. Pea aphid promotes amino acid metabolism both in *Medicago truncatula* and bacteriocytes to favor aphid population growth under elevated CO_2. *Global Change Biology* **19**: 3210–3223.

Heidrich K, Blanvillain-Baufumé S, Parker JE. 2012. Molecular and spatial constraints on NB-LRR receptor signaling. *Current Opinion in Plant Biology* **15**: 385–391.

Hellens RP, Edwards EA, Leyland NR, Bean S, Mullineaux PM. 2000. pGreen: a versatile and flexible binary Ti vector for Agrobacterium-mediated plant transformation. *Plant Molecular Biology* **42**: 819–832.

Hogenhout SA, Bos JI. 2011. Effector proteins that modulate plant–insect interactions. *Current Opinion in Plant Biology* **14**: 422–428.

IPCC. 2013. Observations: atmosphere and surface. In: Stocker T, Qin D, Plattner G, Tignor M, Allen S, Boschung J, Nauels A, Xia Y, Bex B, Midgley B, eds. *Climate change 2013: the physical science basis. Contribution of working group I to the fifth assessment report of the intergovernmental panel on climate change*. Cambridge, UK & New York, NY, USA: Cambridge University Press.

Jaouannet M, Rodriguez PA, Thorpe P, Lenoir CJ, MacLeod R, Escudero-Martinez C, Bos JI. 2014. Plant immunity in plant–aphid interactions. *Frontiers in Plant Science* **5**: 663.

Kaloshian I, Yaghoobi J, Liharska T, Hontelez J, Hanson D, Hogan P, Jesse T, Wijbrandi J, Simons G, Vos P. 1998. Genetic and physical localization of the root-knot nematode resistance locus *Mi* in tomato. *Molecular and General Genetics MGG* **257**: 376–385.

Kanvil S, Powell G, Turnbull C. 2014. Pea aphid biotype performance on diverse *Medicago* host genotypes indicates highly specific virulence and resistance functions. *Bulletin of Entomological Research* **104**: 689–701.

Kissoudis C, van de Wiel C, Visser RG, van der Linden G. 2014. Enhancing crop resilience to combined abiotic and biotic stress through the dissection of physiological and molecular crosstalk. *Frontiers in Plant Science* **5**: 207.

Klingler J, Creasy R, Gao L, Nair RM, Calix AS, Jacob HS, Edwards OR, Singh KB. 2005. Aphid resistance in *Medicago truncatula* involves antixenosis and phloem-specific, inducible antibiosis, and maps to a single locus flanked by NBS-LRR resistance gene analogs. *Plant Physiology* **137**: 1445–1455.

Klingler J, Powell G, Thompson GA, Isaacs R. 1998. Phloem specific aphid resistance in *Cucumis melo* line AR 5: effects on feeding behaviour and performance of *Aphis gossypii*. *Entomologia Experimentalis et Applicata* **86**: 79–88.

Leather SR, Dixon AFG. 1984. Aphid growth and reproductive rates. *Entomologia experimentalis et applicata* **35**: 137–140.

Li P, Ainsworth EA, Leakey AD, Ulanov A, Lozovaya V, Ort DR, Bohnert HJ. 2008. Arabidopsis transcript and metabolite profiles: ecotype-specific responses to open-air elevated [CO_2]. *Plant, Cell & Environment* **31**: 1673–1687.

Liu J-Z, Horstman HD, Braun E, Graham MA, Zhang C, Navarre D, Qiu W-L, Lee Y, Nettleton D, Hill JH. 2011. Soybean homologs of MPK4 negatively regulate defense responses and positively regulate growth and development. *Plant Physiology* **157**: 1363–1378.

Mang H-G, Qian W, Zhu Y, Qian J, Kang H-G, Klessig DF, Hua J. 2012. Abscisic acid deficiency antagonizes high-temperature inhibition of disease resistance through enhancing nuclear accumulation of resistance proteins SNC1 and RPS4 in Arabidopsis. *Plant Cell* **24**: 1271–1284.

Martin P, Johnson SN. 2011. Evidence that elevated CO_2 reduces resistance to the European large raspberry aphid in some raspberry cultivars. *Journal of Applied Entomology* **135**: 237–240.

Mewis I, Appel HM, Hom A, Raina R, Schultz JC. 2005. Major signaling pathways modulate Arabidopsis glucosinolate accumulation and response to both phloem-feeding and chewing insects. *Plant Physiology* **138**: 1149–1162.

Mewis I, Tokuhisa JG, Schultz JC, Appel HM, Ulrichs C, Gershenzon J. 2006. Gene expression and glucosinolate accumulation in *Arabidopsis thaliana* in response to generalist and specialist herbivores of different feeding guilds and the role of defense signaling pathways. *Phytochemistry* **67**: 2450–2462.

Nishizawa-Yokoi A, Tainaka H, Yoshida E, Tamoi M, Yabuta Y, Shigeoka S. 2010. The 26S proteasome function and Hsp90 activity involved in the regulation of HsfA2 expression in response to oxidative stress. *Plant and Cell Physiology* **51**: 486–496.

Nombela G, Williamson VM, Muñiz M. 2003. The root-knot nematode resistance gene *Mi-1.2* of tomato is responsible for resistance against the whitefly *Bemisia tabaci*. *Molecular Plant-Microbe Interactions* **16**: 645–649.

Pieterse CM, Van der Does D, Zamioudis C, Leon-Reyes A, Van Wees SC. 2012. Hormonal modulation of plant immunity. *Annual Review of Cell and Developmental Biology* **28**: 489–521.

Pritchard J, Griffiths B, Hunt EJ. 2007. Can the plant-mediated impacts on aphids of elevated CO_2 and drought be predicted? *Global Change Biology* **13**: 1616–1629.

Qin J, Gu F, Liu D, Yin C, Zhao S, Chen H, Zhang J, Yang C, Zhan X, Zhang M. 2013. Proteomic analysis of elite soybean Jidou17 and its parents using iTRAQ-based quantitative approaches. *Proteome Science* **11**: 12.

Ratcliffe RH, Safranski GG, Patterson FL, Ohm HW, Taylor PL. 1994. Biotype status of Hessian fly (Diptera: Cecidomyiidae) populations from the eastern United States and their response to 14 Hessian fly resistance genes. *Journal of Economic Entomology* **87**: 1113–1121.

Robinson EA, Ryan GD, Newman JA. 2012. A meta-analytical review of the effects of elevated CO_2 on plant–arthropod interactions highlights the importance of interacting environmental and biological variables. *New Phytologist* **194**: 321–336.

Schulze-Lefert P. 2004. Plant immunity: the origami of receptor activation. *Current Biology* **14**: R22–R24.

Song H, Zhao R, Fan P, Wang X, Chen X, Li Y. 2009. Overexpression of *AtHsp90.2*, *AtHsp90.5* and *AtHsp90.7* in *Arabidopsis thaliana* enhances plant sensitivity to salt and drought stresses. *Planta* **229**: 955–964.

Stuart JJ, Chen M-S, Shukle R, Harris MO. 2012. Gall midges (*Hessian flies*) as plant pathogens. *Annual Review of Phytopathology* **50**: 339–357.

Sun YC, Guo HJ, Zhu-Salzman K, Ge F. 2013. Elevated CO_2 increases the abundance of the peach aphid on Arabidopsis by reducing jasmonic acid defenses. *Plant Science* **210**: 128–140.

Tjallingii WF, Hogen-Esch T. 1993. Fine structure of aphid stylet routes in plant tissues in correlation with EPG signals. *Physiological Entomology* **18**: 317–328.

Tsuda K, Katagiri F. 2010. Comparing signaling mechanisms engaged in pattern-triggered and effector-triggered immunity. *Current Opinion in Plant Biology* **13**: 459–465.

Vannette RL, Hunter MD. 2011. Genetic variation in expression of defense phenotype may mediate evolutionary adaptation of *Asclepias syriaca* to elevated CO_2. *Global Change Biology* **17**: 1277–1288.

Walker GP. 2000. A beginner's guide to electronic monitoring of homopteran probing behavior. In: Walker GP, Backus EA, eds. *Principles and applications of electronic monitoring and other techniques in the study of homopteran feeding behavior. Thomas Say Publications in Entomology*. Lanham, MD, USA: Entomological Society of America, 14–40.

Wang R, Zhang Y, Kieffer M, Yu H, Kepinski S, Estelle M. 2016. HSP90 regulates temperature-dependent seedling growth in Arabidopsis by

stabilizing the auxin co-receptor F-box protein TIR1. *Nature Communications* 7: 10269.

Williamson VM. 1998. Root-knot nematode resistance genes in tomato and their potential for future use. *Annual Review of Phytopathology* **36**: 277–293.

Zavala JA, Nabity PD, DeLucia EH. 2013. An emerging understanding of mechanisms governing insect herbivory under elevated CO_2. *Annal Review of Entomology* **58**: 79–97.

Zhang M, Botër M, Li K, Kadota Y, Panaretou B, Prodromou C, Shirasu K, Pearl LH. 2008. Structural and functional coupling of Hsp90-and Sgt1-centred multi-protein complexes. *EMBO Journal* **27**: 2789–2798.

Zhu Y, Qian W, Hua J. 2010. Temperature modulates plant defense responses through NB-LRR proteins. *PLoS Pathogens* **6**: e1000844.

Zhu-Salzman K, Salzman RA, Ahn J-E, Koiwa H. 2004. Transcriptional regulation of sorghum defense determinants against a phloem-feeding aphid. *Plant Physiology* **134**: 420–431.

Supporting Information

Additional Supporting Information may be found online in the Supporting Information tab for this article:

Table S1 Primer sequences used for real-time quantitative PCR

Table S2 Changes in protein profile of *Medicago truncatula* A17 genotype in response to aphid infestation under ambient CO_2

Table S3 Changes in protein profile of *Medicago truncatula* Jester in response to aphid infestation under ambient CO_2

Table S4 Changes in protein profile of *Medicago truncatula* A17 in response to aphid infestation under elevated CO_2

Table S5 Changes in protein profile of *Medicago truncatula* Jester in response to aphid infestation under elevated CO_2

Please note: Wiley Blackwell are not responsible for the content or functionality of any Supporting Information supplied by the authors. Any queries (other than missing material) should be directed to the *New Phytologist* Central Office.